Available online at www.sciencedirect.com
ScienceDirect
Journal of the European Ceramic Society 30 (2010) 1237–1243
www.elsevier.com/locate/jeurceramsoc

More on the microstructural characterization of dense particle gels

Anett Wagner [a,*], Markus Hütter [b], Dietrich Stoyan [c]

[a] *Institute for Geotechnics, TU Bergakademie Freiberg, Gustav-Zeuner-Strasse 1, Freiberg D-09596, Saxony, Germany*
[b] *Polymer Physics, Department of Materials, ETH Zurich, Zurich CH-8093, Switzerland*
[c] *Institute for Stochastics, TU Bergakademie Freiberg, Freiberg D-09596, Germany*

Received 12 February 2009; received in revised form 17 September 2009; accepted 8 October 2009
Available online 27 November 2009

Abstract

A systematic study of the microstructure of densely packed coagulated colloidal particle gels is important for understanding their macroscopic, in particular, mechanical properties. It was previously shown that heterogeneous gels exhibit higher elastic properties and yield strengths than their homogeneous counterparts at the same solids loading. This was explained by the newly developed straight path method.[1] However, this macroscopic behaviour can be also explained by classical and conceptually simpler methods of spatial statistics, in particular, the pair-correlation function and the related *K*-function. Additionally, the structural differences of homogeneous and heterogeneous gels can be described by the contact distributions, which characterize the pore space and are of relevance for certain transport properties. The understanding of the structural differences is completed by presenting a benchmark model, which is in some sense 'between' the homogeneous and heterogeneous case.

Keywords: A. Suspensions; B. Grain size; B. Microstructure-prefiring

1. Introduction

It is well known that the microstructure of materials determines in a high degree their macroscopic properties,[2,3] e.g., the mechanical properties in terms of elastic modulus and yield strength. Therefore it is important to control the microstructure, for which a fundamental condition is characterization. For the latter, successful methods have been developed in spatial statistics.[2,4,5]

There are two classes of these characterization methods. The first, perhaps most natural, is based on analyses of the objects that form the structures. In the case considered here, the 'objects' are hard spheres. If the spheres are identical, the approach in essence analyses the system of centres, i.e., spatial point patterns, and uses point process methods.[6] With some modification the same is possible when the spheres can intersect and have variable diameters. Statistical summary characteristics such as pair-correlation function,[2,4,6,7] Ripley's *K*-function[6] and bond angle distribution,[7] triangle distribution function,[7] common neighbour distribution,[1] dihedral angle distribution[1] and straight path analysis[1] are then appropriate tools. They all characterize in various ways the relative positions of the spheres or objects.

The second approach is set-theoretic and considers the set-theoretic union of the objects, which is then treated as a sample of a random set. The methods of statistics for random sets[4] lead to statistical summary characteristics of a nature quite different from those of the object-oriented approach. They are able to characterize the system of the pores outside the objects. Since in the case of spherical objects the pore space is totally connected, any attempt to characterize pores as single objects with size and shape is difficult. Set-theoretic characteristics such as the so-called contact distributions are then more natural, which characterize the pore space from the position of random test points. Further set-theoretic characteristics are the Minkowski functionals[4] and the *k*-point probability functions.[2]

We mention that there is a third approach for the statistical characterization of structures as discussed in the present paper, namely the tessellation approach.[8,9] It is based on spatial tessellations constructed for the systems of spheres, which are in the case of identical spheres the well-known Voronoi tessellations.

In the present paper only the simplest characteristics of the first two approaches are used, with the aim to show that already these lead to valuable and new structural statements for par-

* Corresponding author. Tel.: +49 3731 394079; fax: +49 3731 393638.
E-mail address: Anett.Wagner@ifgt.tu-freiberg.de (A. Wagner).

0955-2219/$ – see front matter © 2009 Elsevier Ltd. All rights reserved.
doi:10.1016/j.jeurceramsoc.2009.10.004

ticle gels as obtained in the colloidal processing of ceramic materials.[10] The method called Direct Coagulation Casting[11] (DCC) allows one to destabilize the colloidal suspension in two distinct ways, rather homogeneously throughout the sample. The double layer repulsion between particles is diminished by either changing in situ the pH in the solvent (ΔpH-method) or by increasing in situ the ionic strength (ΔI-method). It has been shown by Brownian dynamics computer simulations[7,12] that the corresponding structure of the evolving particle network is rather homogeneous (called 'hom' in the following) and heterogeneous (called 'het' in the following), respectively.

In the analysis of these structures, various classical characterization methods were applied, namely the pair-correlation function,[7] the bond angle distribution,[7] and the Minkowski functions in conjunction with the parallel-body technique.[13] Additionally, the triangle distribution function,[7] the common neighbour distribution,[1] the dihedral angle distribution[1] and the straight path method[1] were used. The latter method was particularly designed in order to prove the existence of some quasi-linear arrangement of load-bearing particle chains,[1] which is of relevance for the mechanical properties, e.g., elastic properties and yield strength. This method, however, depends on a distance parameter, which must be chosen by the investigator.

The present paper aims at demonstrating the power of classical, conceptually simpler methods, for which commercial software exists. These methods yield additional information about the microstructure of the simulated ceramic materials. It uses again the pair-correlation function, but its interpretation is supported by the so-called K-function in order to understand the arrangement of the spheres in very short distances. Additionally, the pore space is explored by means of the contact distributions. For better understanding, the analysis of the structures 'hom' and 'het' introduced above is discussed in relation to a third simulated, benchmark, structure. The latter is called 'fba' (force-biased algorithm, see below) and is discussed in more detail in the following.

2. Materials and methods

2.1. The structures

The two structures 'hom' and 'het' are random systems of identical impenetrable spheres (diameter d) of volume fraction 40%. Both structures are the result of Brownian dynamics simulations[7,12] of the colloidal particles, mimicking the coagulation of the suspension. To that end, two physical effects are taken into account: on the one hand, DLVO-forces consisting of van der Waals attraction and electrostatic double layer repulsion, and on the other hand, Brownian forces as a result of the thermal kicks of the solvent molecules. By changing the repulsive interaction in a way representative of the ΔpH- or the ΔI-method in DCC, the different network structures 'hom' and 'het' emerged as the coagulated structure. One may consider these structures as random, if the term 'random' is understood in the way like Torquato uses it in his book[2] for 'random heterogeneous' media or structures.

For the purpose of comparison, a third structure is considered, which is generated according to different principles. The comparison structure 'fba' is also a structure with hard spheres of a volume fraction of 40%, but one generated with an algorithm which aims to simulate systems with neither attraction nor repulsion between the spheres. The algorithm, called force-biased algorithm[6,14] is a so-called collective rearrangement algorithm. It starts with a completely random configuration of identical spheres in an epipedal container, where overlappings of the spheres are permitted. During the algorithm the spheres are shifted in order to reduce the overlaps and in parallel the radii are reduced stepwise. When a structure of non-interpenetrating spheres is obtained, it is rescaled in order to have the diameters wanted. Experience shows that after short computation time a random system of hard spheres of a prescribed volume fraction V_V is obtained, if $V_V < 0.66$. Note that also higher volume fractions are possible, but it takes more computing time to simulate such packings; the generation of packings of $V_V = 0.4$ is quite easy.

The statistical analyses of the present paper are based on samples of 8.000 spheres all of diameter $d = 1.0$, in a cubical container, with periodic boundary conditions.

2.2. Structure characterization methods

2.2.1. Visual inspection

The simplest step of structural analysis is visual inspection of substructures. At this point, we wish to emphasize the following. Very often in discussion of structure–property relations, the structure is specified by providing a picture of a sample cross-section as obtained by some experimental technique[1] or by a snapshot of a simulation.[7] As the human brain is highly optimized in recognizing patterns, such efforts may be justified. However, one should always aspire to find quantitative measures for discussing the structure. Therefore, we just briefly mention the visual inspection here, before we will extent earlier quantitative methods.

Schenker et al.[1] consider in their Fig. 1 micrographs obtained by cryo-SEM to gain a first optical impression of the structures. The present paper uses thin slices of a thickness of two sphere diameters. Fig. 1 shows vertical projections of such slices for 'hom', 'het' and 'fba'.

2.2.2. Contact distributions

The contact distributions characterize in some way the size and shape of the pore space outside the hard spheres, by considering it in the set-theoretic sense. The most important types are the linear and spherical contact distributions.[4]

The linear contact distribution is defined as follows. Choose a random point in the pore space and go from this point in a given (prescribed) direction until the first contact with the surface of a sphere occurs. The prescribed direction may be that in the positive or the negative direction of the x-axis. This yields a random length, the probability density function of which is denoted by $h_\ell(r)$. It is important to know that the linear contact distribution is closely related to the chord length distribution.[4] This is the distribution of the lengths of line segments lying completely

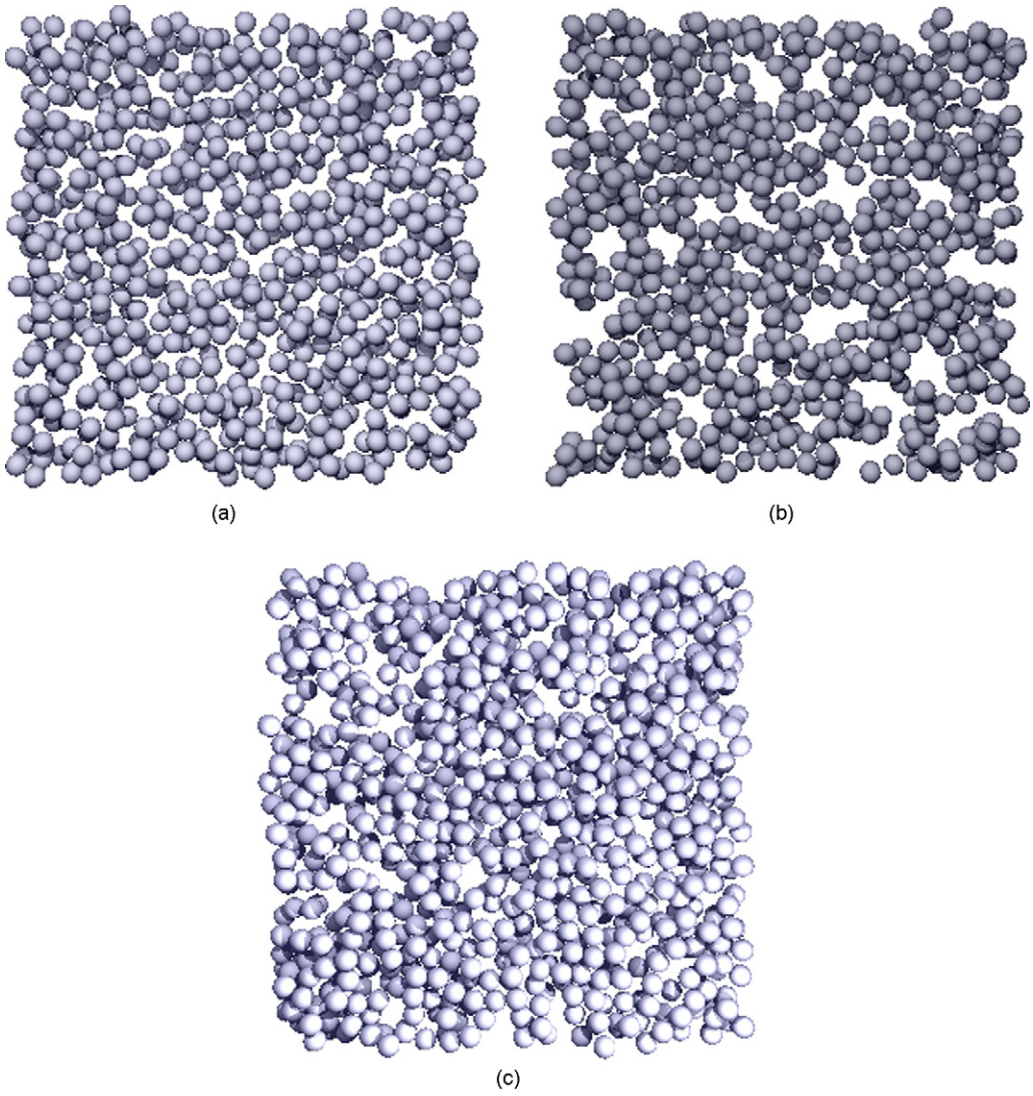

Fig. 1. Vertical projections of slices of thickness $2d$ for the structures 'hom' (a), 'het' (b) and 'fba' (c), respectively.

outside the spheres occurring when an infinitely long line of arbitrary orientation intersects the packing of spheres. In particular, the mean chord length m_L (which is the mean of the chord length distribution) and the probability density function $h_\ell(r)$ are related by[4]

$$h_\ell(0) = \frac{1}{m_L}. \tag{1}$$

For statistically homogeneous and isotropic systems of identical non-overlapping (i.e., hard) spheres of diameter d and volume fraction V_V, m_L is given by[4]

$$m_L = \frac{2(1 - V_V)}{3V_V} d, \tag{2}$$

irrespective of the specific arrangement.

The linear contact distribution characterizes the linear extent of the pores. It plays an important role in the study of relationships between microstructure and macroscopic transport properties.[2]

Statistical experience[15] and physical arguments[16] show that for many systems of hard spheres, especially for systems in equilibrium, natural packed systems and systems simulated with the force-biased algorithm, the probability density function of the linear contact distribution can be well approximated by an exponential function, i.e.

$$h_\ell(r) = \frac{1}{\lambda} \exp\left(-\frac{r}{\lambda}\right) \quad \text{for } r \geq 0. \tag{3}$$

Since the exponential distribution depends only on one parameter, λ gives the complete 'linear' information. If the linear contact distribution is really an exponential distribution, then the parameter is given by

$$\lambda = \frac{1}{m_L}. \tag{4}$$

The definition of the spherical contact distribution is similar to that of the linear contact distribution. Again, a random test point in the pore space is chosen, but now it is the centre of a growing sphere. Its radius in the case of first contact with one

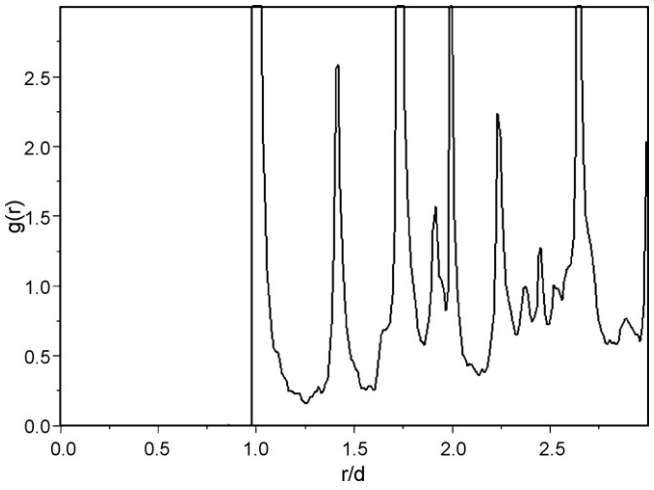

Fig. 2. The pair-correlation function for a random dense sphere packing of volume fraction $V_V = 0.70$. The peaks correspond to frequently appearing distances between pairs of spheres.

of the hard spheres is the random variable of interest; in other words, the distance from the random point to the nearest spheres surface point. The corresponding probability density function is $h_s(r)$. It is noted that $h_s(r)$ can be transformed in the Minkowski functional $W_1(r)$ in Ref. 14 and the corresponding distribution function is closely related to $W_0(r)$ there. It can be shown that for any statistically homogeneous and isotropic arrangement of non-overlapping particles

$$h_s(0) = \frac{S_V}{1 - V_V}, \tag{5}$$

where S_V is the specific surface content.[4] In the particular case of identical hard spheres of diameter d one can use the relation

$$S_V = \frac{6V_V}{d}. \tag{6}$$

For many hard sphere systems, natural packings and such obtained by the force-biased algorithm, it turns out that the spherical contact distribution can be well approximated by the so-called half normal distribution[15]

$$h_s(r) = \frac{2}{\sqrt{2\pi}\sigma} \exp\left\{-\frac{r^2}{2\sigma^2}\right\} \quad \text{for} \quad r \geq 0. \tag{7}$$

The corresponding mean is

$$m_s = \sqrt{\frac{2}{\pi}}\sigma = \frac{2}{\pi}\frac{1}{h_s(0)}. \tag{8}$$

2.2.3. Pair-correlation function

The pair-correlation function $g(r)$ is a well-known means for the characterization of particle arrangements,[2,4,6,7] describing the frequency of distances between particle centres. For later interpretation, it may be useful to consider the pair-correlation function for a random dense sphere packing of volume fraction $V_V = 0.70$ as shown in Fig. 2.

In Fig. 2, r is the distance between the sphere centres and d their diameter. As the volume fraction is rather high and above that of random close packing ($V_V = 0.64$), the structure shows partly crystalline behaviour. This leads to the strong peaks at $r/d = 1$, $\sqrt{2}$, $\sqrt{3}$ and 2, which correspond to characteristic distances in hexagonally packed sphere arrangements.

2.2.4. Ripley's K-function

Ripley's K-function[6] or the integrated pair-correlation function, $K(r)$, is related to the pair-correlation function by

$$K(r) = 4\pi \int_0^r s^2 g(s)\,\mathrm{d}s.$$

Its statistical interpretation is as follows. If ρ_0 denotes the mean number of particles per unit volume, then $\rho_0 K(r)$ is the average number of particle centres within range r of another particle centre. In the context of the present paper, the K-function is helpful in the finer analysis of the poles of the pair-correlation function.

3. Results and discussion

3.1. Qualitative visual inspection

The three projected slices in Fig. 1 show qualitatively clear structural differences between 'hom' and 'het', and show that 'fba' is indeed 'between' both in a structural sense. The structure 'hom' has longish pores and the arrangement of the spheres is not so dense, often there are small gaps in between. In contrast 'het' has larger, rounder pores and the spheres form dense clusters, i.e., the structure is more heterogeneous. Probably, the most relevant difference between the two structures with influence on the macroscopic mechanical properties is the structure of the clusters of spheres; the different pore structure seems to be a logical consequence.

3.2. Contact distributions

The qualitative impression with respect to the pore structure resulting from visual inspection is quantitatively confirmed in Figs. 3 and 4. Both contact distributions indicate larger pores for 'het', both in the linear and spherical sense. The structure 'fba' is well between the originally given structures.

As shown in Fig. 3, the histogram of the sample for the 'fba' sample of the linear contact distribution follows well the theoretical exponential distribution where the parameter $\lambda = 1/m_L$ is determined with m_L according to (2) and (4). In contrast, the histogram for 'hom' shows that there are more short distances between the test points and the sphere surfaces, while 'het' has more longer distances. The means $\bar{\ell}$ behave in the same way. The mean for 'fba' is close to the value 1 as expected by (2) and (4).

The spherical contact distribution functions behave similarly. The histograms are shown in Fig. 4 together with the approximation by the half normal distribution given by formula (7). The theoretical value for $h_s(0)$ is 4, according to (5) and (6). Again, the histogram for 'fba' is well fitted by the half normal distribution, while in 'hom' there are more short distances between the test points and the sphere surfaces, and in 'het' there are more long distances.

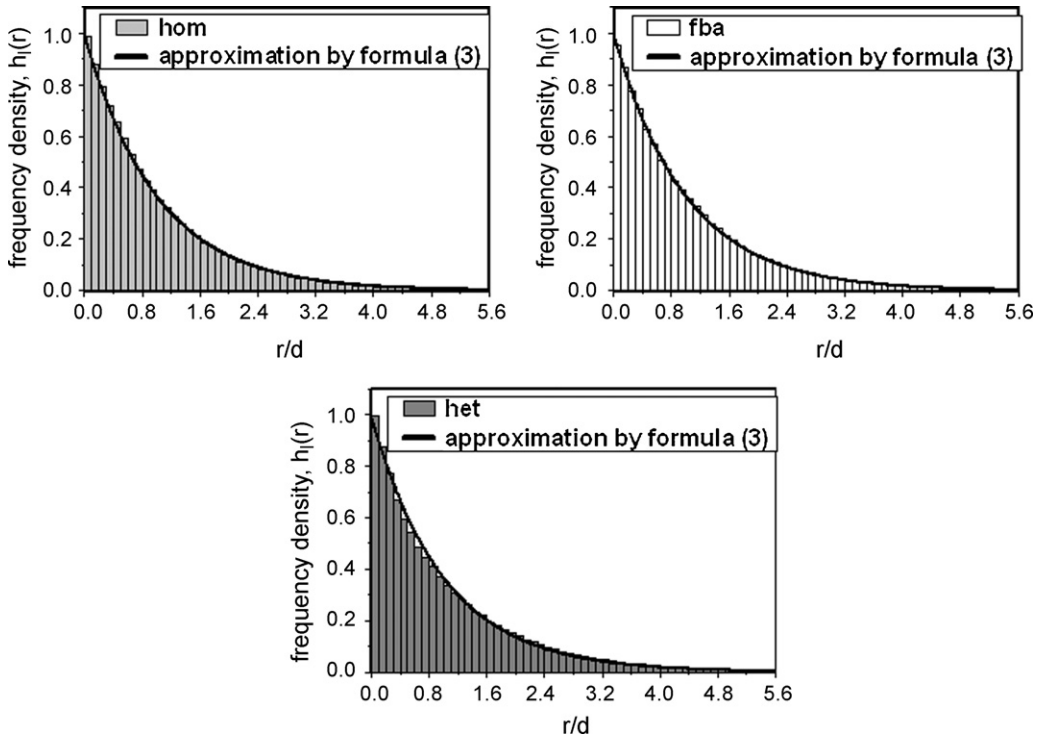

Fig. 3. The histograms of the linear contact distribution for 'hom', 'fba' and 'het' as well as the approximation by the exponential distribution (formula (3) with $\lambda = 1/m_L$ and m_L by formula (2)), respectively.

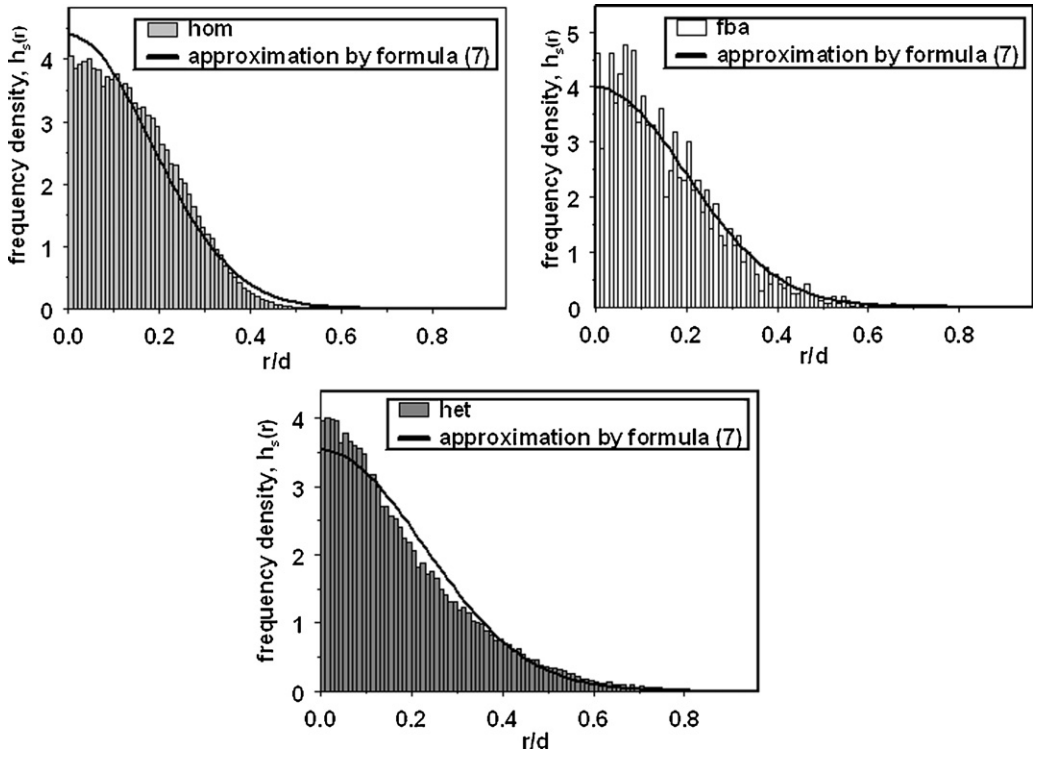

Fig. 4. The histograms of the spherical contact distribution for the three structures 'hom', 'fba' and 'het' as well as the approximation by the half normal distribution (formula (7) with σ obtained by (5)–(7)), respectively.

Table 1
The means $\bar{\ell}$ and $\bar{s}$ of the linear and spherical contact distributions for the three structures.

Structure	$\bar{\ell}$	$\bar{s}$
'hom'	0.971	0.145
'fba'	1.023	0.152
'het'	1.074	0.180

This results in analogous differences of the means $\bar{s}$ as shown in Table 1. The mean for 'fba' is close to the value $1/(2\pi) \approx 0.159$ as expected from (5) and (8).

3.3. Pair-correlation function

The pair-correlation functions of the three structures shown in Fig. 5 differ clearly; again 'fba' takes an intermediate position. All pair-correlation functions have a pole at $r/d = 1.0$ resulting from spheres in contact or in very short distance. However, it is difficult to use the curves in Fig. 5 to get information about the 'strength' of the peaks, on the number of pairs of spheres which contribute.

The structure 'het' has a further peak at $r/d \cong 1.08$, which is quite unusual for hard sphere systems but can be explained physically.[13] It seems to correspond to pairs of spheres close together but with a little gap between due to a secondary minimum in the interaction potential. The next peak of 'het' appears at $r/d = 2.0$. It corresponds to straight chains of three spheres. Since the peak for 'het' is larger than for 'hom', one can conclude that such chains appear in 'het' more frequently than in 'fba'.

The pair-correlation function for 'hom' is quite different: there is only a small extra peak at $r/d \cong 1.08$, but two weak local maxima at $r/d \cong \sqrt{2}$ (this is in a simple cubic unit cell, the length of a face diagonal) and $\sqrt{3}$ (this is in a simple cubic unit cell, the length of a body diagonal) and the peak at $r/d = 2.0$ is less pronounced as compared to 'het' and 'fba'. By the way, neither 'hom' nor 'het' has a maximum at $r/d = 3.0$, indicating that there are no linear chains of four particles.

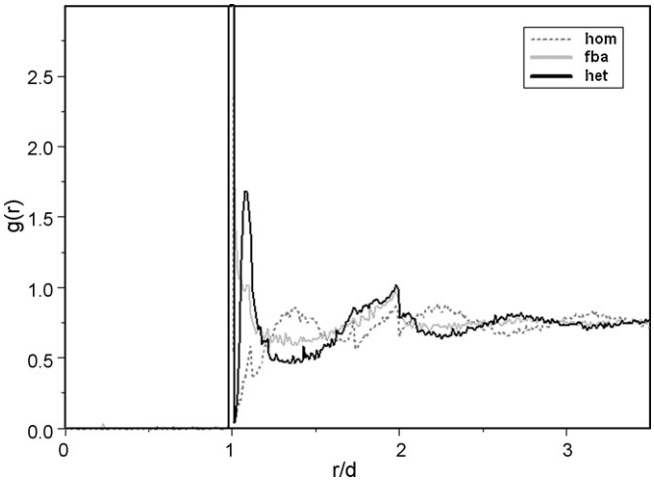

Fig. 5. The pair-correlation functions of the three structures. Note that the peaks at $r/d = 1.0$ coincide for 'hom' and 'fba'.

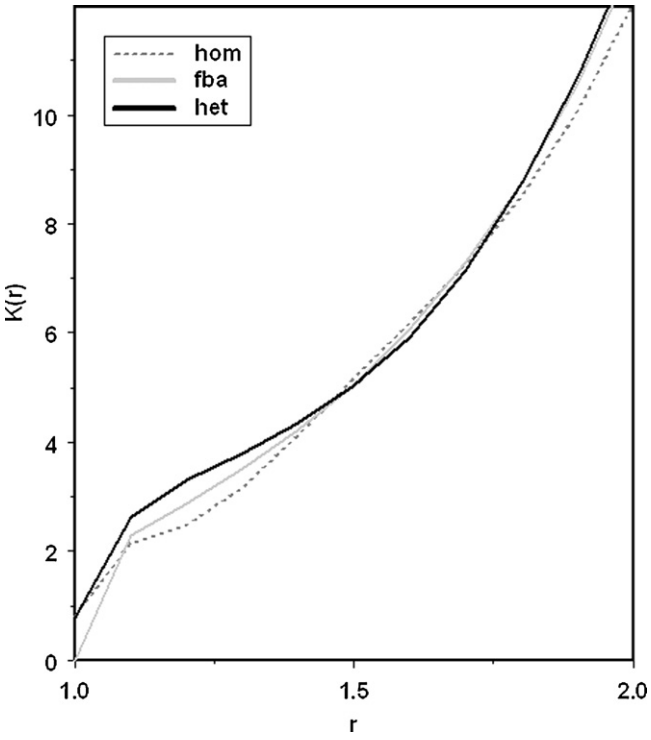

Fig. 6. The K-functions for 'hom', 'het' and 'fba'.

3.4. K-function

The K-functions for the three structures are shown in Fig. 6.

The curves explain the nature of the behaviour of $g(r)$ at $r/d = 1.0$: The number of spheres in direct contact (or very close together) is nearly equal for 'hom' and 'het', while it is zero for 'fba'. Thus the strength of the poles at $r = 0$ is equal for 'hom' and 'het'.

Second, they show that in 'het' there are more pairs of spheres close together than in 'hom'. This cannot be explained by the peak at $r/d \cong 1.08$ alone, only the knowledge of $K(r)$ for r between 1 and 1.08 yields this information. The values of $K(1.1)$–$K(1.0)$ in Table 2 show very clearly that indeed the 1.08 pairs appear additionally.

Third, there are also clear differences in the numbers of sphere centres of a distance between $1.9 \leq r/d \leq 2.1$. As the peak of the pair-correlation function at $r/d \cong 2.0$ indicates, it should be greatest for 'het'. This is shown clearer and confirmed by the values of $K(2.1)$–$K(1.9)$ in Table 2.

Table 2
$K(1.1)$–$K(1.0)$ (In the case of 'hom' and 'het' the value $K(1.1)$–$K(0.99)$, i.e., the minimum of the pair-correlation function.) and $K(2.1)$–$K(1.9)$ for the three structures.

Structure	$K(1.1)$–$K(1.0)$	$K(2.1)$–$K(1.9)$
'hom'	1.340	3.931
'fba'	2.288	4.211
'het'	1.817	4.436

4. Conclusions

This paper presents various tools for the quantification of structural differences of dense particle gels. The analysis is improved by introducing a null model or benchmark structure generated by a force-biased algorithm ('fba'). The characteristics include the contact distributions, the pair-correlation function, and the K-function. All these characteristics avoid to use any additional parameter such as the threshold angle θ_c which must be subjectively chosen.

By means of these three methods (contact distributions, pair-correlation function, and K-function) clear structural differences between 'het' and 'hom' have been observed. The additionally used intermediate structure 'fba' shows in a fine way the extremal structural properties of 'het' and 'hom'. The contact distribution functions show that 'het' has larger pores, which means that the spheres in this structure form denser clusters. This may be a first way to explain the higher mechanical strength of this structure.

The pair-correlation function gives valuable information on the topology of the systems of hard spheres. It is able to show some tendency of forming chains of particles in the different structures, by the peaks at $r/d = 1.0$, 1.08 and 2.0. Ripley's K-function helps to understand the true geometrical structure of the sphere systems.

It is interesting to compare the results of the pair-correlation function analysis with those of the straight path analysis.[1] The pair-correlation function yields information on absolutely straight chains of spheres and finds only chains of two or three members; their number is larger in 'het' than in 'hom'. Additionally it shows that the peak at $r/d \cong 1.08$ is significant for the structure 'het', i.e., this structure has more pairs of spheres lying close together than 'hom'. These topological properties may well be responsible for the higher strength of 'het'. The straight path method[1] instead considers chains with small angles between the vectors connecting the sphere centres; these chains can be longer than three. This was the main argument in Schenker et al. for explanation of the higher strength of 'het'. In view of characterizing the differences between various structures with respect to the mechanical properties, our method is distinct from the one proposed by Schenker et al. in two respects. First, we do not make use of an artificial (cut-off) parameter. And, second, our method makes use of a *standard* structural quantifier, $g(r)$ (and the directly related Ripley K-function), known to the scientific community for a long time. Although it is usually argued that the pair-correlation information is not sufficient to describe the gel structure, it must be pointed out that the behaviour of $K(r)$ for small r leads to important conclusions about the absolute number of force-transmitting direct contacts between particles.

References

1. Schenker, I., Filser, F. T., Aste, T. and Gauckler, L. J., Microstructures and mechanical properties of dense particle gels: microstructural characterisation. *J. Eur. Ceram. Soc.*, 2008, **28**, 1443–1449.
2. Torquato, S., *Random Heterogeneous Materials: Microstructure and Macroscopic Properties*. Springer, New York, 2002.
3. Sahimi, M., *Flow and Transport in Porous Media and Fractured Rock: Form Classical Methods to Modern Approaches*. Wiley VCH-Verlag GmbH, 1995.
4. Stoyan, D., Kendall, W. S. and Mecke, J., *Stochastic Geometry and Its Application* (*2nd ed.*). J. Wiley, Chichester, 1995.
5. Ohser, J. and Mücklich, F., *Statistical Analysis of Microstructure in Material Science*. J. Wiley, Chichester, 2000.
6. Illian, J., Penttinnen, A., Stoyan, H. and Stoyan, D., *Statistical Analysis and Modelling of Spatial Point Patterns*. J. Wiley, Chichester, 2008.
7. Hütter, M., Local structure evaluation in particle network formation studied by Brownian dynamics simulation. *J. Colloid Interface Sci.*, 2000, **231**, 150–337.
8. Sastry, S., Corti, D. S., Debenedetti, P. G. and Stillinger, F. H., Statistical geometry of particle packings: I. Algorithm for exact determination of connectivity. Volume and surface areas of void space in mono- and polydisperse sphere packings. *Phys. Rev. E*, 1997, **56**, 5524–5532.
9. Sastry, S., Debenedetti, P. G. and Stillinger, F. H., Statistical geometry of particle packings: II. 'Weak Spots' in liquids. *Phys. Rev. E*, 1997, **56**, 5533–5543.
10. Lange, F. F., Colloidal processing of powder for reliable ceramics. *Curr. Opin. Solid State Mater. Sci.*, 1998, **3**, 496–500.
11. Graule, T. J., Baader, F. H. and Gauckler, L. J., Enzyme catalysis of ceramic forming. *J. Mater. Educ.*, 1994, **16**, 243–267.
12. Hütter, M., Brownian dynamics simulation of stable and of coagulating colloids in aqueous suspensions, Ph.D. Thesis No. 13107, ETH Zurich, Switzerland, 1999. http://e-collection.ethz.ch/show?type=diss&nr=13107.
13. Hütter, M., Heterogeneity of colloidal particle networks analysed by means of Minkowski functionals. *Phys. Rev. E*, 2003, **68**, 031404.
14. Bezrukov, A., Stoyan, D. and Bargiel, M., Statistical analysis for simulated random packings of spheres. *Part. Part. Syst. Charact.*, 2002, **19**, 111–118.
15. Stoyan, D., Wagner, A., Hermann, H. and Elsner, A., Statistical characterisation of the pore space of random systems of hard spheres. *J. Non-Cryst. Solids*, under review.
16. Binglin, L. and Torquato, S., Lineal-path function for random heterogeneous materials. *Phys. Rev. A*, 1992, **45**, 922–929.